Inorganic Chemistry
Article

Inorg. Chem. **2010**, *49*, 7007–7015 **7007**
DOI: 10.1021/ic100886x

Li^+, Cu^+, and Ag^+ Oligonuclear Structures with the Sterically Demanding Bis(3,5-tertbutylpyrazol-1-yl)dithioacetate Heteroscorpionate Ligand

Irene Bassanetti, Marcello Gennari, Luciano Marchiò,* Mattia Terenghi, and Lisa Elviri

Dipartimento di Chimica Generale ed Inorganica, Chimica Analitica, Chimica Fisica, Università degli Studi di Parma, viale G. P. Usberti 17/a, I 43100 Parma, Italy

Received May 5, 2010

The heteroscorpionate N_2S_2 donor ligand bis(3,5-tertbutylpyrazol-1-yl)dithioacetate (L) was prepared as a Li^+ trinuclear complex, which co-crystallizes with tetrahydrofuran (THF) solvent molecules: $[Li(L)]_3 \cdot (2.25)THF$. When $[Li(L)]_3$ was reacted with $AgBF_4$ or $[Cu(CH_3CN)_4]BF_4$, the oligonuclear species $[Ag(L)]_3$ and $[Cu_5(L)_4]BF_4$ were isolated and structurally characterized. The Ag^+ complex presents an irregular trinuclear structure in which three AgL moieties define a central trigonal site that may potentially host a fourth metal ion. The Cu^+ complex exhibits a highly symmetric pentanuclear structure in which four equivalent CuL moieties shape an internal tetrahedral site occupied by an additional Cu^+ ion. According to electrospray-mass spectrometry (ESI-MS) and ^1H diffusion NMR spectroscopy, the Ag^+ and Cu^+ complexes maintain oligonuclear structures in solution. In particular, the Cu^+ pentanuclear complex, once dissolved, rapidly equilibrates with the tetranuclear species $[Cu_4(L)_3]^+$. This is confirmed by the presence of two sets of NMR signals, which demonstrated a change in ratio at different complex concentrations effected by a NMR dilution titration. Variable temperature NMR experiments (210−303 K) defined the activation parameters associated with the fluxional behavior of $[Cu_5(L)_4]BF_4$ and $[Cu_4(L)_3]^+$, and these results are consistent with intramolecular rearrangements in both species ($\Delta S^{\ddagger} < 0$).

Introduction

Scorpionate ligands[1,2] are a versatile class of compounds that have found applications in many research fields, including catalysis,[3−5] bioinorganic chemistry,[6−10] magnetism,[11−13] and supramolecular chemistry.[14−16] The first member of this class of compounds is the hydrotris(pyrazolyl)borate anion (Tp),[17] in which the three nitrogen atoms can occupy a trigonal face of a coordination polyhedron.[18] Throughout the years, a number of modifications have been contrived to tune the donor ability of Tp, which primarily consist of (a) the introduction of steric hindrance on the pyrazole rings and (b) the replacement of pyrazole with other moieties bearing different donor atoms from nitrogen.[19−33] The evolution of the coordination properties of the B-centered scorpionates has been paralleled by that of the C-centered scorpionates. In

*To whom correspondence should be addressed. E-mail: marchio@unipr.it.

(1) Trofimenko, S. *Scorpionates-The coordination chemistry of polypyrazolylborate ligands*; Imperial College Press: London, 1999.
(2) Pettinari, C. *Scorpionate II, chelating borate ligands*; Imperial College Press: London, 2008.
(3) Slugovc, C.; Padilla-Martinez, I.; Sirol, S.; Carmona, E. *Coord. Chem. Rev.* **2001**, *213*, 129–157.
(4) Vetter, A. J.; Flaschenriem, C.; Jones, W. D. *J. Am. Chem. Soc.* **2005**, *127*, 12315–12322.
(5) Vetter, A. J.; Rieth, R. D.; Brennessel, W. W.; Jones, W. D. *J. Am. Chem. Soc.* **2009**, *131*, 10742–10752.
(6) Parkin, G. *Chem. Rev.* **2004**, *104*, 699–767.
(7) Melnick, J. G.; Parkin, G. *Science* **2007**, *317*, 225–227.
(8) Kitajima, N.; Fukui, H.; Morooka, Y.; Mizutani, Y.; Kitagawa, T. *J. Am. Chem. Soc.* **1990**, *112*, 6402–6403.
(9) Kitajima, N.; Fujisawa, K.; Tanaka, M.; Morooka, Y. *J. Am. Chem. Soc.* **1992**, *114*, 9232–9233.
(10) Seebacher, J.; Shu, M. H.; Vahrenkamp, H. *Chem. Commun.* **2001**, 1026–1027.
(11) Reger, D. L.; Gardinier, J. R.; Elgin, J. D.; Smith, M. D.; Hautot, D.; Long, G. J.; Grandjean, F. *Inorg. Chem.* **2006**, *45*, 8862–8875.
(12) Janiak, C. *Chem. Ber.* **1994**, *127*, 1379–1385.
(13) Hamon, P.; Mari, A.; Meunier, J. F.; Toupet, L.; Cador, O.; Etienne, M.; Hamon, J. R. *Inorg. Chim. Acta* **2009**, *362*, 4389–4395.
(14) Janiak, C.; Hemling, H. *J. Chem. Soc., Dalton. Trans.* **1994**, 2947–2952.
(15) Janiak, C.; Temizdemir, S.; Dechert, S. *Inorg. Chem. Commun.* **2000**, *3*, 271–275.
(16) Reger, D. L.; Gardinier, J. R.; Bakbak, S.; Semeniuc, R. F.; Bunz, U. H. F.; Smith, M. D. *New J. Chem.* **2005**, *29*, 1035–1043.
(17) Trofimenko, S. *J. Am. Chem. Soc.* **1966**, *88*, 1842–1844.
(18) Parkin, G. *Chem. Commun.* **2000**, 1971–1985.
(19) Reglinski, J.; Spicer, M. D.; Garner, M.; Kennedy, A. R. *J. Am. Chem. Soc.* **1999**, *121*, 2317–2318.
(20) Benkmil, B.; Ji, M.; Vahrenkamp, H. *Inorg. Chem.* **2004**, *43*, 8212–8214.
(21) Shu, M. H.; Walz, R.; Wu, B.; Seebacher, J.; Vahrenkamp, H. *Eur. J. Inorg. Chem.* **2003**, 2502–2511.
(22) Kimblin, C.; Hascall, T.; Parkin, G. *Inorg. Chem.* **1997**, *36*, 5680–5681.
(23) Gardinier, J. R.; Silva, R. M.; Gwengo, C.; Lindeman, S. V. *Chem. Commun.* **2007**, 1524–1526.
(24) Silva, R. M.; Gwengo, C.; Lindeman, S. V.; Smith, M. D.; Gardinier, J. R. *Inorg. Chem.* **2006**, *45*, 10998–11007.
(25) Minoura, M.; Landry, V. K.; Melnick, J. G.; Pang, K. L.; Marchio, L.; Parkin, G. *Chem. Commun.* **2006**, 3990–3992.
(26) Bailey, P. J.; Lanfranchi, M.; Marchio, L.; Parsons, S. *Inorg. Chem.* **2001**, *40*, 5030–5035.

Published on Web 07/06/2010

Scheme 1. Ligand Synthesis

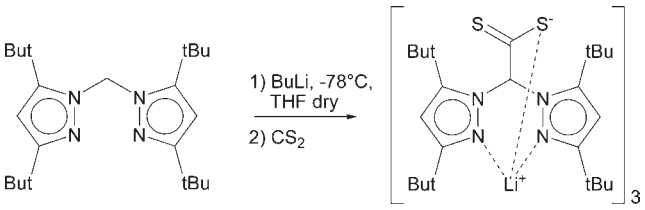

particular, C-centered heteroscorpionate ligands have been prepared that exhibit Cp,[34] phenol/alcohol,[35−38] thioether,[39−41] or a carboxyl and thiocarboxyl[42−44] residues in addition to the N_2 donor system. Furthermore, polytopic ligands designed to produce supramolecular architectures have also been described.[45−47]

In the present work, we have studied the coordination properties of the C-centered heteroscorpionate ligand bis(3,5-tertbutylpyrazol-1-yl)dithioacetate (L, Scheme 1). Homologous ligands have been previously reported, and their binding properties were assessed mainly with early transition metals and in the presence of co-ligands.[44,48] Because the chemistry of this class of scorpionates has been little explored, we wish to extend the investigation concerning the coordination capabilities of L with late transition metals, which are likely to exploit the affinity of the dithioacetate groups for *soft* metal ions, such as Cu^+ and Ag^+. The presence of the dithioacetate group renders this ligand potentially N_2S_2 tetradentate because both sulfur atoms can be involved in metal binding for this moiety. Furthermore, the bispyrazole (N_2) and dithioacetate (S_2) donor systems are linked by the tetrahedral central carbon atom, which introduces divergent binding sites at an angle of ∼109°. These features represent the main reason for the formation of oligonuclear complexes with Li^+, Cu^+, and Ag^+. In addition, the presence of bulky *t*-Bu groups on the pyrazole rings provides additional steric and hydrophobic protection to the central core of these homoleptic complexes.

Because the X-ray structures of $[Li(L)]_3$, $[Ag(L)]_3$, and $[Cu_5(L)_4]BF_4$ indicate that L tends to support oligomers (through S-bridging), we wished to investigate the nuclearity of these species in solution. This study was performed by means of electrospray-mass (ESI-MS) spectrometry[49−51] combined with dilution, diffusion,[52−54] and variable temperature ^{1}H NMR experiments. The silver complex occurs in solution as a trinuclear entity whereas the copper complex exhibits a pentanuclear-tetranuclear equilibrium. According to the X-ray characterization, the disposition of the ML units in the oligonuclear structures provides a central cavity that may host an additional metal ion. In the silver complex, the shape of this cavity is suitable for a relatively small cation favoring a trigonal planar geometry, whereas in the copper complex, the tetrahedral central site is already occupied by a Cu^+ ion. The possibility that mixed MM′L ($M = Cu^+$, $M' = Ag^+$) complexes may form was further explored with ESI-MS spectrometry.

Experimental Section

General Procedures. 3,5-Di-*tert*-butylpyrazole was obtained from 2,2,6,6-tetramethyl-3,5-heptanedione and hydrazine hydrate using a reported literature method.[55] Bis(3,5-*t*-butylpyrazol-1-yl)methane was prepared according to the general method employed for the synthesis of bis(pyrazolyl)methanes via reaction of azoles with CH_2Cl_2 under phase transfer catalysis conditions.[56,57] $[Cu(CH_3CN)_4]BF_4$ was prepared as previously described.[58] All other reagents and solvents were commercially available. Tetrahydrofuran (THF) and MeOH were distilled over Na/benzophenone and CaH_2, respectively, and carbon disulfide was stored over 3 Å molecular sieves before use. The syntheses were performed under inert gas (N_2) using Schlenk techniques. Single crystals of the complexes were obtained in a glovebox (N_2). Infrared spectra were recorded from 4000 to 700 cm^{-1} on a Perkin-Elmer FT-IR Nexus spectrometer equipped with a Smart Orbit HATR accessory (diamond crystal). ^{1}H NMR spectra were recorded on a Bruker Avance

(27) Cammi, R.; Gennari, M.; Giannetto, M.; Lanfranchi, M.; Marchio, L.; Mori, G.; Paiola, C.; Pellinghelli, M. A. *Inorg. Chem.* **2005**, *44*, 4333–4345.
(28) Janiak, C.; Scharmann, T. G.; Albrecht, P.; Marlow, F.; Macdonald, R. *J. Am. Chem. Soc.* **1996**, *118*, 6307–6308.
(29) Chiou, S. J.; Ge, P. H.; Riordan, C. G.; Liable-Sands, L. M.; Rheingold, A. L. *Chem. Commun.* **1999**, 159–160.
(30) Mutseneck, E. V.; Bieller, S.; Bolte, M.; Lerner, H. W.; Wagner, M. *Inorg. Chem.* **2010**, *49*, 3540–3552.
(31) Ge, P. H.; Haggerty, B. S.; Rheingold, A. L.; Riordan, C. G. *J. Am. Chem. Soc.* **1994**, *116*, 8406–8407.
(32) Qin, Y.; Cui, C. Z.; Jakle, F. *Macromolecules* **2008**, *41*, 2972–2974.
(33) Lu, C. C.; Peters, J. C. *Inorg. Chem.* **2006**, *45*, 8597–8607.
(34) Otero, A.; Fernandez-Baeza, J.; Antinolo, A.; Tejeda, J.; Lara-Sanchez, A.; Sanchez-Barba, L.; Rodriguez, A. M.; Maestro, M. A. *J. Am. Chem. Soc.* **2004**, *126*, 1330–1331.
(35) Hoffman, J. T.; Carrano, C. J. *Inorg. Chim. Acta* **2006**, *359*, 1248–1254.
(36) Otero, A.; Fernandez-Baeza, J.; Antinolo, A.; Tejeda, J.; Lara-Sanchez, A.; Sanchez-Barba, L.; Rodriguez, A. M. *Eur. J. Inorg. Chem.* **2004**, 260–266.
(37) Higgs, T. C.; Carrano, C. J. *Inorg. Chem.* **1997**, *36*, 291–297.
(38) Gennari, M.; Tegoni, M.; Lanfranchi, M.; Pellinghelli, M. A.; Marchio, L. *Inorg. Chem.* **2007**, *46*, 3367–3377.
(39) Zhang, J.; Braunstein, P.; Hor, T. S. A. *Organometallics* **2008**, *27*, 4277–4279.
(40) Hammes, B. S.; Carrano, C. J. *Chem. Commun.* **2000**, 1635–1636.
(41) Gennari, M.; Tegoni, M.; Lanfranchi, M.; Pellinghelli, M. A.; Giannetto, M.; Marchio, L. *Inorg. Chem.* **2008**, *47*, 2223–2232.
(42) Otero, A.; Fernandez-Baeza, J.; Tejeda, J.; Antinolo, A.; Carrillo-Hermosilla, F.; Diez-Barra, E.; Lara-Sanchez, A.; Fernandez-Lopez, M.; Lanfranchi, M.; Pellinghelli, M. A. *J. Chem. Soc., Dalton Trans.* **1999**, 3537–3539.
(43) Burzlaff, N.; Hegelmann, I.; Weibert, B. *J. Organomet. Chem.* **2001**, *626*, 16–23.
(44) Otero, A.; Fernandez-Baeza, J.; Antinolo, A.; Carrillo-Hermosilla, F.; Tejeda, J.; Lara-Sanchez, A.; Sanchez-Barba, L.; Fernandez-Lopez, M.; Rodriguez, A. M.; Lopez-Solera, I. *Inorg. Chem.* **2002**, *41*, 5193–5202.
(45) Reger, D. L.; Gardinier, J. R.; Semeniuc, R. F.; Smith, M. D. *J. Chem. Soc., Dalton Trans.* **2003**, 1712–1718.
(46) Reger, D. L.; Sirianni, E.; Horger, J. J.; Smith, M. D.; Semeniuc, R. F. *Cryst. Growth Des.* **2010**, *10*, 386–393.
(47) Reger, D. L.; Semeniuc, R. F.; Smith, M. D. *Eur. J. Inorg. Chem.* **2002**, 543–546.
(48) Pellei, M.; Alidori, S.; Camalli, M.; Campi, G.; Lobbia, G. G.; Mancini, M.; Papini, G.; Spagna, R.; Santini, C. *Inorg. Chim. Acta* **2008**, *361*, 1456–1462.
(49) Spasojevic, I.; Boukhalfa, H.; Stevens, R. D.; Crumbliss, A. L. *Inorg. Chem.* **2001**, *40*, 49–58.
(50) Algarra, A. G.; Basallote, M. G.; Fernandez-Trujillo, M. J.; Guillamon, E.; Llusar, R.; Segarra, M. D.; Vicent, C. *Inorg. Chem.* **2007**, *46*, 7668–7677.
(51) Collins, J. M.; Uppal, R.; Incarvito, C. D.; Valentine, A. M. *Inorg. Chem.* **2005**, *44*, 3431–3440.
(52) Macchioni, A.; Ciancaleoni, G.; Zuccaccia, C.; Zuccaccia, D. *Chem. Soc. Rev.* **2008**, *37*, 479–489.
(53) Pregosin, P. S. *Prog. Nucl. Magn. Reson. Spectrosc.* **2006**, *49*, 261–288.
(54) Zuccaccia, D.; Macchioni, A. *Organometallics* **2005**, *24*, 3476–3486.
(55) Yang, G. A.; Raptis, R. G. *Inorg. Chim. Acta* **2003**, *352*, 98–104.
(56) Juliá, S.; Sala, P.; Del Mazo, J.; Sancho, M.; Ochoa, C.; Elguero, J.; Fayet, J. P.; Vertut, M. C. *J. Heterocyclic Chem.* **1982**, *19*, 1141–1145.
(57) Beck, A.; Weibert, B.; Burzlaff, N. *Eur. J. Inorg. Chem.* **2001**, 521–527.
(58) Leftin, J. H. *Chem. Abstr.* **1967**, *66*, 46487e.

Table 1. Summary of X-ray Crystallographic Data for $[Li(L)]_3\cdot(2.25)THF$, $[Cu_5(L)_4]BF_4$, and $[Ag(L)]_3$

	$[Li(L)]_3\cdot(2.25)THF$	$[Cu_5(L)_4]BF_4$	$[Ag(L)]_3$
empirical formula	$C_{81}H_{135}Li_3N_{12}O_{2.25}S_6$	$C_{96}H_{156}BCu_5F_4N_{16}S_8$	$C_{72}H_{117}Ag_3N_{12}S_6$
formula weight	1526.19	2195.36	1666.75
color, habit	orange, block	red, prism	red, prism
crystal size, mm	$0.23 \times 0.18 \times 0.15$	$0.37 \times 0.22 \times 0.20$	$0.45 \times 0.35 \times 0.20$
crystal system	monoclinic	tetragonal	triclinic
space group	$C2/c$	$I\bar{4}$	$P\bar{1}$
a, Å	27.095(1)	20.830(3)	15.396(2)
b, Å	15.709(1)	20.830(3)	15.833(2)
c, Å	46.906(2)	13.270(2)	21.295(3)
α,deg.	90	90	68.871(2)
β, deg.	110.35(1)	90	83.645(3)
γ, deg.	90	90	61.547(2)
V, Å^3	18719(2)	5758(2)	4245(1)
Z	8	2	2
T, K	293(2)	293(2)	173(2)
ρ (calc), Mg/m^3	1.083	1.266	1.304
μ, mm^{-1}	0.193	1.108	0.877
θ range, deg.	1.52 to 24.72	1.38 to 26.53	1.51 to 27.90
no. of rflcn/obsv	15986/10161	5981/5055	19567/13098
GoF	1.019	1.007	1.006
$R1^a$	0.0594	0.0377	0.0323
$wR2^a$	0.1461	0.0964	0.0596

^{a} $R1 = \sum||F_o| - |F_c||/\sum|F_o|$, $wR2 = [\sum w(F_o^2 - F_c^2)^2/\sum w(F_o^2)^2]^{1/2}$, $w = 1/[\sigma^2(F_o^2) + (aP)^2 + bP]$, where $P = [\max(F_o^2,0) + 2F_c^2]/3$.

300 spectrometer using standard Bruker pulse sequences. Chemical shifts are reported in parts per million (ppm) referenced to residual solvent protons. Elemental analyses (C, H, N) were performed with a Carlo Erba EA 1108 automated analyzer.

Synthesis of $[Li(L)]_3\cdot(2.25)THF$. *n*-BuLi (6 mL, 1.6 M in hexane, 9.60 mmol) was slowly added to a solution of bis(3,5-*t*-butylpyrazol-1-yl)methane (3.13 g, 8.40 mmol) in THF (100 mL) at −78 °C. After stirring the orange solution for 15 min, carbon disulfide (0.60 mL, ρ = 1.266 g/cm^3, 9.98 mmol) was slowly added, and the resulting deep red solution was allowed to warm to room temperature with stirring. After 3 h, the solvents were removed in vacuo, and the residue was washed with hexane (2 × 15 mL), dried and collected as a pale orange powder ($[Li(L)]_3\cdot(2.25)THF$, 2.6 g, 1.70 mmol, 61%). IR (cm^{-1}): ∼3300 m, br (H_2O), 2960 m, 2905 m, 2871 m, 1650 m, 1541 m, 1463 m, 1364 m, 1319 m, 1253 m, 1228 m, 1088s, 1060s, 1007s, 878s, 853s. ^{1}H NMR (300 MHz, $CDCl_3$) δ 1.21 (s, 18H, CH_3), 1.43 (s, 18H, CH_3(*t*-Bu), 1.89 (m, 4H, CH_2(THF)), 3.82 (m, 4H, OCH_2-(THF)), 5.96 (s, 2H, CH pz), 7.07 (s, 1H, $CH_{central}$). According to the intensities of the signals the THF content is consistent with ∼2.2 molecules for each $[Li(L)]_3$ complex. Anal. Calcd for $C_{72}H_{117}N_{12}S_6Li_3$ 2.25THF (1526.24): C, 63.74; H, 8.91; N, 11.01. Found: C, 63.31; H, 8.49; N, 11.48. Dark orange single crystals suitable for X-ray data collection were obtained by layering hexane over a THF solution of the product, which corresponded to $[Li(L)]_3\cdot(2.25)THF$.

Synthesis of $[Cu_5(L)_4](BF_4)$. A solution of $[Cu(CH_3CN)_4]BF_4$ (420 mg, 1.33 mmol) in MeOH (30 mL) was added to a solution of $[Li(L)]_3\cdot(2.25)THF$ (500 mg, 0.328 mmol) in MeOH (10 mL), and a dark brown precipitate was formed. After 0.5 h, the solution was filtered, washed with MeOH (5 mL), dried and collected ($[Cu_5L_4](BF_4)$, 465 mg, 0.212 mmol, 86%). IR (cm^{-1}): 2953s, 2904w, 2855w, 1534 m, 1452 m, 1364s, 1321w, 1255 m, 1222s, 1079s, 1052vs, 1014s, 794s. ^{1}H NMR (300 MHz, CD_2Cl_2, 230 K): δ 0.94−1.36 (m br, 36H, CH_3), 5.94 (s, 1H, CH pz), 6.01 (s, 1H, CH pz), 7.43 (s, 1H, $CH_{central}$). Anal. Calcd. for $C_{96}H_{156}N_{16}S_8Cu_5BF_4$ (2195.44): C, 52.52; H, 7.16; N, 10.21. Found: C, 52.26; H, 6.70; N, 9.95. ESI-MS (p.i., CH_3OH, m/z, I%): 1597.68, 34 $[Cu_4(L)_3]^+$; 2107.90, 100 $[Cu_5(L)_4]^+$. Dark red single crystals suitable for X-ray data collection were obtained by layering hexane over a solution of the product in CH_2Cl_2.

Synthesis of $[Ag(L)]_3$. $[Li(L)]_3\cdot(2.25)THF$ (223 mg, 0.146 mmol) and $AgBF_4$ (90 mg, 0.462 mmol), were dissolved in MeOH (15 mL), and the initial red solution yielded a red precipitate. After 15 min, the mixture was filtered, washed with MeOH (5 mL), dried and collected ($[Ag(L)]_3$, 160 mg, 0.096 mmol, 66%). IR (cm^{-1}): 2962s, 2904w, 2871w, 1545 m, 1458 m, 1361s, 1319w, 1252 m, 1228s, 1105 m, 1084 m, 1064 m, 992s, 875w, 851w, 798vs, 750s. ^{1}H NMR (300 MHz, $(CD_3)_2CO$, 300 K): δ 1.29 (s, 18H, CH_3), 1.41 (s, 18H, CH_3), 6.16 (s, 2H, CH pz), 7.86 (s, 1H, $CH_{central}$). Anal. Calcd. for $C_{72}H_{117}N_{12}S_6Ag_3$ (1666.78): C, 51.88; H, 7.07; N, 10.08. Found: C, 51.62; H, 6.93; N, 9.94. ESI-MS (p.i., CH_3OH, m/z, I%): 1666.33, 12 $[Ag(L)]_3^+$; 1689.25, 100 $[Ag(L)]_3Na^+$, 1705.25, 32 $[Ag(L)]_3K^+$, 1773.42, 7 $[Ag_4(L)_3]^+$. Red crystals suitable for X-ray data collection were obtained by layering MeOH over a CH_2Cl_2 solution of the product at −18 °C.

X-ray Crystallography. A summary of data collection and structure refinement for $[Li(L)]_3\cdot(2.25)THF$, $[Cu_5(L)_4]BF_4$, and $[Ag(L)]_3$ is reported in Table 1. Single crystal data were collected with a Bruker Smart 1000 and with a Bruker Smart APEXII area detector diffractometers (Mo Kα; λ = 0.71073 Å). Cell parameters were refined from the observed setting angles and detector positions of selected strong reflections. Intensities were integrated from several series of exposure frames that covered the sphere of reciprocal space.[59] An absorption correction was applied using the program SADABS[60] with minimum and maximum transmission factors of 0.845−1.000 ($[Li(L)]_3\cdot(2.25)$-THF), 0.865−1.000 ($[Cu_5(L)_4]BF_4$) and 0.663−1.000 ($[Ag(L)]_3$). The structures were solved by direct methods (SIR97)[61] and refined with full-matrix least-squares (SHELXL-97)[62] using the Wingx software package.[63] Non-hydrogen atoms were refined anisotropically, and the hydrogen atoms were placed at their calculated positions. The crystals of $[Li(L)]_3\cdot(2.25)THF$ were grown from a THF solution, and one molecule of this solvent of crystallization was found disordered in three positions with site occupancy factors of 0.33 for each fragment. Another molecule of THF was located on a binary axis and was refined with a site occupancy factor of 0.25. Ortep diagrams

(59) *SMART* (*control*) *and SAINT* (*integration*) *software for CCD systems*; Bruker AXS: Madison, WI, 1994.
(60) *Area-Detector Absorption Correction*; Siemens Industrial Automation Inc.: Madison, WI, 1996.
(61) Altomare, A.; Burla, M. C.; Camalli, M.; Cascarano, G. L.; Giacovazzo, C.; Guagliardi, A.; Moliterni, A. G. G.; Polidori, G.; Spagna, R. *J. Appl. Crystallogr.* **1999**, *32*, 115–119.
(62) Sheldrick, G. M. *SHELX97, Programs for Crystal Structure Analysis*, Release 97−2; University of Göttingen: Göttingen, Germany, 1997.
(63) Farrugia, L. J. *J. Appl. Crystallogr.* **1999**, *32*, 837–838.

were prepared using the ORTEP-3[64] and Mercury 2.0[65] programs. CCDC 773133−773135 contains the supplementary crystallographic data for this paper.

ESI-MS experiments. An LTQ XL linear ion trap mass spectrometer (Thermo Electron Corporation, San Josè, CA) equipped with an ESI/API Ion Max source was used. The ESI source was connected to a solvent delivery system (Finnigan Surveyor, MS Pump Plus) that was used to pump a continuous flow of methanol (200 μL min^{-1}). Instrumental tuning was performed by direct infusion of a freshly prepared methanolic solution (1 nM) of pure $[Cu_5(L)_4]BF_4$ into the continuous flow of methanol from the pump. The most abundant ion at m/z 2108, which corresponds to the $[Cu_5(L)_4]^+$ metal cluster, was used to optimize source ionization efficiency and lens ion transmission. Working parameters were set as follows: spray voltage, 3.5 kV; capillary voltage, 15 V; capillary temperature, 200 °C; tube lens, 65 V. Samples were analyzed in flow injection mode by means of a six-port valve equipped with a 2 μL sample loop. Mass spectra were recorded in full scan analysis mode in the range 1000−2500 m/z.

For titration experiments of $[Cu_5(L)_4]BF_4$ with $AgBF_4$, six solutions were prepared in methanol and incubated at room temperature for 15 h; each solution contained a fixed concentration of $[Cu_5(L)_4]BF_4$ (50 μM) and an increasing concentration of $AgBF_4$ (20, 40, 60, 80, 100, 250 μM), which resulted in final $[Ag^+]/[[Cu_5(L)_4]BF_4]$ ratios of 0.40, 0.85, 1.30, 1.70, 2.10, and 5.30, respectively.

PGSE Measurements. ^{1}H PGSE (pulsed gradient spin echo) NMR measurements were performed for $[Ag(L)]_3$ and for a mixture of $[Cu_4(L)_3]^+/[Cu_5(L)_4]^+$ (ratio 1/0.6) in CD_2Cl_2. A standard stimulated echo (STE) sequence on a Bruker Avance 300 spectrometer was employed (room temperature without spinning). The most intense signals were taken into account during the data processing. The dependence of the resonance intensity (I) on the gradient strength (g) is described by the following equation:

$$I = I_0 e^{-D\gamma^2 g^2 \delta^2 (\Delta - \delta/3)}$$

where I = observed intensity (attenuated signal intensity), I_0 = reference intensity (unattenuated signal intensity), D = diffusion coefficient, γ = nucleus gyromagnetic ratio, g = gradient strength, δ = gradient duration, and Δ = diffusion delay. The parameters δ (1.6 ms) and Δ (60 ms) were kept constant during the experiments, whereas g was varied from 2 to 95% in 16 steps. All spectra were acquired using 16 K points and processed with a line broadening of 1.0 Hz. PGSE data were treated by applying a procedure reported in the literature,[54] which uses an internal standard (tetrakis(trimethylsilyl)silane, TMSS; r_H^{TMSS} (hydrodynamic radius) $\approx r_{vdW}^{TMSS}$ (van der Waals radius) = 4.28 Å).[66] The van der Waals volume (V_{vdW})[67] and the solvent-excluded volume (V_{SE})[68] of $[Ag(L)]_3$ and $[Cu_5(L)_4]BF_4$ were computed from the atomic coordinates derived using X-ray geometries. The X-ray volumes ($V_{X\text{-}ray}$) were computed by dividing the unit cell volume by the number of oligonuclear entities contained in the unit cell. Because there is no crystallization solvent for $[Ag(L)]_3$ and $[Cu_5(L)_4]BF_4$, this latter procedure should provide reliable values for the molecular volume.

Results and Discussion

The synthesis of L follows a reported procedure,[69] based on the reaction between differently substituted bis(pyrazol-1-yl)methanes and butyl lithium in THF followed by treatment with CS_2 at low temperature (Scheme 1). The heteroscorpionate ligands previously prepared according to this method include bis(3,5dimethylpyrazol-1-yl)dithioacetate and bis-(3,5diphenylpyrazol-1-yl)dithioacetate. These ligands have been employed primarily with early transition metals, such as Ti, Y, and Sc, and they behave as N_2S donors that form mononuclear complexes.[44,70,71] The coordination capabilities of L are virtually identical to those of the aforementioned heteroscorpionates, but the increased steric hindrance provided by the *t*-Bu residues is expected to affect the geometry of the resulting complexes. The lithium complex crystallizes as a trinuclear species $[Li(L)]_3$, whereas the less hindered bis(3,5diphenylpyrazol-1-yl)dithioacetate ligand affords a mononuclear complex in the presence of adventitious water. The formation of oligomeric structures with Li^+ is not new for this type of ligand; the bis(3,5dimethylpyrazol-1-yl)-acetate ligand (N_2O donor) has also yielded a tetranuclear complex.[44] Treatment of $[Li(L)]_3$ with 3 equiv of $AgBF_4$ yielded a trinuclear $[Ag(L)]_3$ complex. The same reaction was attempted with Cu^+ by treating $[Li(L)]_3$ with 3 equiv of $[Cu(CH_3CN)_4]BF_4$; however, the pentanuclear $[Cu_5(L)_4]BF_4$ complex precipitated from the reaction mixture. The synthesis was optimized by using a slight excess of copper (Cu/L ratio of 1.3), which is consistent with the 5/4 Cu/L ratio reported in the X-ray structure. As discussed in the ^{1}H NMR section (vide infra), the $[Cu_5(L)_4]BF_4$ complex is in equilibrium with a $[Cu_4(L)_3]^+$ tetranuclear entity in CD_2Cl_2 solution. The propensity to generate oligonuclear species appears to be characteristic of L, arising from (a) the bridging ability of the thioacetate group, (b) the steric hindrance in the form of *t*-Bu residues, and (c) the absence of ancillary ligands. The Cu^+ and Ag^+ complexes are dark red air-stable solids that are soluble in common organic solvents.

Solid-State Structures. Relevant geometric parameters for $[Li(L)]_3 \cdot (2.25)THF$, $[Cu_5(L)_4]BF_4$, and $[Ag(L)]_3$ are reported in Tables 2−4, and the molecular structures of the three compounds are depicted in Figures 1−3. The Li^+ complex is trinuclear, and each metal is surrounded by two nitrogen and two sulfur atoms, which define a Li_3S_3 ring that is in a chair conformation (Figure 1). Each ligand chelates in the N_2S coordination mode on one metal and bridges a second metal with the same sulfur atom. The other sulfur atom does not participate in metal chelation and points outside the Li_3S_3 hexa-atomic ring. The Li−N bond distances are not equivalent; one bond is significantly longer than the other (Table 2). This inequivalence is also observed for the Li−S distances; the $Li-S_{chelate}$ is significantly longer than the $Li-S_{bridge}$ (~0.06 Å). The metal geometry can be described as trigonal pyramidal with the metal residing in the coordination plane. Another characteristic feature of the complex is the non-symmetric

(64) Farrugia, L. J. *J. Appl. Crystallogr.* **1997**, *30*, 568.
(65) Macrae, C. F.; Edgington, P. R.; McCabe, P.; Pidcock, E.; Shields, G. P.; Taylor, R.; Towler, M.; van de Streek, J. *J. Appl. Crystallogr.* **2006**, *39*, 453–457.
(66) Dinnebier, R. E.; Dollase, W. A.; Helluy, X.; Kummerlen, J.; Sebald, A.; Schmidt, M. U.; Pagola, S.; Stephens, P. W.; Van Smaalen, S. *Acta Crystallogr., Sect B: Struct. Sci.* **1999**, *B55*, 1014–1029.
(67) Bondi, A. *J. Phys. Chem.* **1964**, *68*, 441–451.
(68) V_{SE} takes into account that the cavities and inlets of the solute are not accessible by the solvent so that $V_{SE} > V_{vdW}$. Connolly, M. L. *J. Am. Chem. Soc.* **1985**, *107*, 1118–1124.
(69) Otero, A.; Fernandez-Baeza, J.; Antinolo, A.; Tejeda, J.; Lara-Sanchez, A. *J. Chem. Soc., Dalton Trans.* **2004**, 1499–1510.
(70) Otero, A.; Fernandez-Baeza, J.; Antinolo, A.; Tejeda, J.; Lara-Sanchez, A.; Sanchez-Barba, L.; Rodriguez, A. M. *J. Chem. Soc., Dalton Trans.* **2004**, 3963–3969.
(71) Otero, A.; Fernandez-Baeza, J.; Antinolo, A.; Tejeda, J.; Lara-Sanchez, A.; Sanchez-Barba, L.; Martinez-Caballero, E.; Rodriguez, A. M.; Lopez-Solera, I. *Inorg. Chem.* **2005**, *44*, 5336–5344.

Table 2. Selected Bond Lengths (Å) and Angles (deg) for $[Li(L)]_3 \cdot (2.25)THF$

Li(1)−N(21)	2.077(5)	Li(1)−S(19)	2.539(5)
Li(1)−N(22)	2.130(5)	Li(1)−S(13)	2.580(5)
N(21)−Li(1)−N(22)	87.9(2)	N(21)−Li(1)−S(13)	90.54(19)
N(21)−Li(1)−S(19)	142.8(2)	N(22)−Li(1)−S(13)	91.68(18)
N(22)−Li(1)−S(19)	129.3(2)	S(19)−Li(1)−S(13)	89.59(16)
Li(2)−N(24)	2.073(6)	Li(2)−S(13)	2.535(5)
Li(2)−N(25)	2.144(6)	Li(2)−S(16)	2.620(6)
N(24)−Li(2)−N(25)	88.2(2)	N(24)−Li(2)−S(16)	89.1(2)
N(24)−Li(2)−S(13)	141.7(3)	N(25)−Li(2)−S(16)	91.9(2)
N(25)−Li(2)−S(13)	130.1(3)	S(13)−Li(2)−S(16)	89.39(17)
Li(3)−N(27)	2.109(6)	Li(3)−S(16)	2.535(5)
Li(3)−N(28)	2.144(5)	Li(3)−S(19)	2.606(5)
N(27)−Li(3)−N(28)	87.6(2)	N(27)−Li(3)−S(19)	89.1(2)
N(27)−Li(3)−S(16)	146.3(2)	N(28)−Li(3)−S(19)	92.08(19)
N(28)−Li(3)−S(16)	126.1(2)	S(16)−Li(3)−S(19)	91.24(16)

Table 3. Selected Bond Lengths (Å) and Angles (deg) for $[Cu_5(L)_4]BF_4$

Cu(1)−N(21)	1.970(2)	S(12)−Cu(1)−S(22)′	113.40(3)
Cu(1)−S(12)	2.293(1)	N(21)−Cu(1)−S(12)	106.73(8)
Cu(1)−S(22)′	2.1633(9)	N(21)−Cu(1)−S(22)′	139.88(8)
Cu(1)−N(23)	2.684(3)		
Cu(2)−S(12)	2.3106(8)	S(12)′−Cu(2)−S(12)	106.20(2)
		S(12)′−Cu(2)−S(12)″	116.23(4)

′ = $y-1/2; -x+1/2; -z+1/2$. ″ = $-y+1/2; x+1/2; -z+1/2$.

Table 4. Selected Bond Lengths (Å) and Angles (deg) for $[Ag(L)]_3$

Ag(1)−N(23)	2.421(2)	Ag(1)−S(28)	2.4644(7)
Ag(1)−N(21)	2.523(2)	Ag(1)−S(12)	2.5939(7)
N(23)−Ag(1)−S(28)	132.90(5)	N(23)−Ag(1)−S(12)	86.59(5)
N(23)−Ag(1)−N(21)	72.56(6)	S(28)−Ag(1)−S(12)	130.64(2)
S(28)−Ag(1)−N(21)	127.80(4)	N(21)−Ag(1)−S(12)	86.64(4)
Ag(2)−N(26)	2.399(2)	Ag(2)−S(22)	2.4606(7)
Ag(2)−N(24)	2.616(2)	Ag(2)−S(15)	2.5938(7)
N(26)−Ag(2)−S(22)	147.16(4)	N(26)−Ag(2)−N(24)	69.18(6)
N(26)−Ag(2)−S(15)	89.87(5)	S(22)−Ag(2)−N(24)	125.16(5)
S(22)−Ag(2)−S(15)	116.87(2)	S(15)−Ag(2)−N(24)	90.64(4)
Ag(3)−N(27)	2.344(2)	Ag(3)−S(25)	2.4399(7)
Ag(3)−N(29)	2.622(2)	Ag(3)−S(18)	2.5967(7)
N(27)−Ag(3)−S(25)	137.50(5)	N(27)−Ag(3)−N(29)	73.59(7)
N(27)−Ag(3)−S(18)	95.34(4)	S(25)−Ag(3)−N(29)	126.19(5)
S(25)−Ag(3)−S(18)	123.51(2)	S(18)−Ag(3)−N(29)	78.71(4)

placement of the two pyrazole rings that provide the N_2 system. This placement has consequences for the overall shape of the trinuclear assembly; three *t*-Bu groups located on one side of the Li_3S_3 moiety diverge from the molecular center, whereas the other three *t*-Bu groups on the opposite side of the Li_3S_3 moiety are converging toward the center (Figure 1). In the first case, a hydrophobic pocket is generated that hosts a THF solvent molecule. This is a surprising finding for two reasons: THF, when present, is usually bound to lithium, and Li−S interactions are less common than Li−O bonds.[72] In a previous report, the less sterically hindered bis(3,5-diphenylpyrazol-1-yl)dithioacetate ligand yielded a tetrahedral mononuclear Li^+ complex (N_2O_2 coordination) that lacked interaction of the $-CS_2^-$ moiety with the metal in the presence of THF and adventitious water.[44] In $[Li(L)]_3 \cdot (2.25)THF$, the preference for sulfur over oxygen by the Li^+ atom may plausibly be related to favorable interactions between the hydrophobic pocket formed by the *t*-Bu groups and the appropriately sized THF molecule.

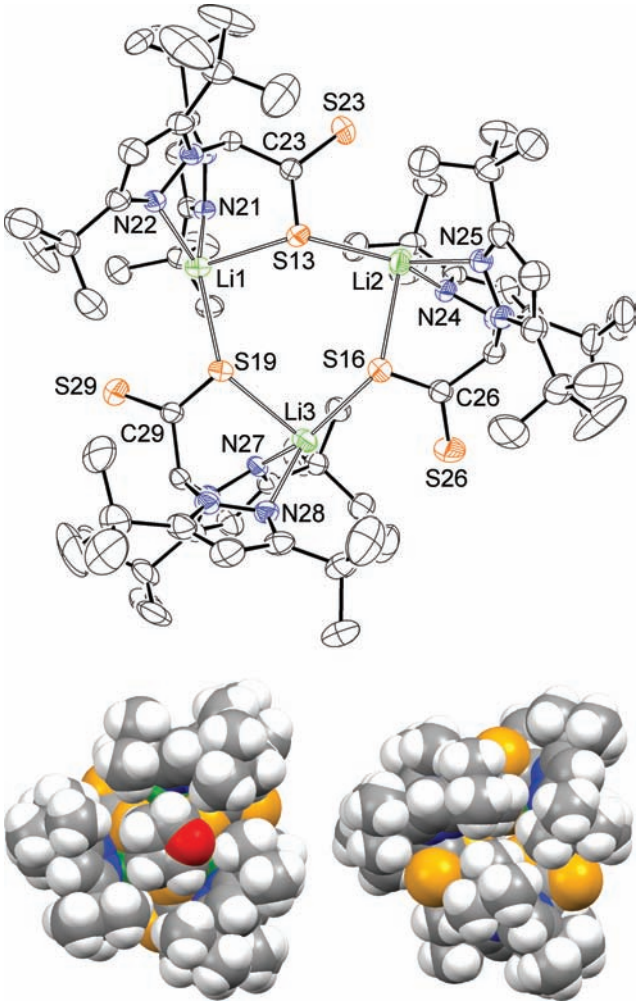

Figure 1. Top, ORTEP drawing of $[Li(L)]_3 \cdot (2.25)THF$ at the 30% thermal ellipsoids probability level. The hydrogen atoms and the crystallization solvent molecules are omitted for clarity. Bottom, a spacefilling representation of $[Li(L)]_3 \cdot (2.25)THF$; top view (left) and bottom view (right).

The copper complex exhibits a pentanuclear structure in which four CuL units provide an internal tetrahedral pocket that is occupied by an additional Cu^+ ion, and the positive charge of the $[Cu_5(L)_4]^+$ moiety is balanced by a BF_4^- anion. The complex crystallizes in the tetragonal $I\bar{4}$ space group, and the asymmetric unit is represented by one CuL entity (Figure 2). Each peripheral metal presents a trigonal planar geometry defined by a nitrogen and a sulfur atom of one ligand and by a bridging sulfur atom of another ligand. The nitrogen atom of one pyrazole ring does not take part in the metal coordination because of a particularly long (2.684(8) Å) Cu−N distance, and the metal is located inside the trigonal plane; the considerable mismatch between the nitrogen lone pair and the copper atom is further evidence that this pyrazole ring is non-coordinating. The metal at the center (Cu(2)) is within a nearly perfect tetrahedral geometry, and the Cu−S bond distances are significantly longer than those of the peripheral copper atoms. The Cu_5S_8 cluster is surrounded by a hydrophobic shield provided by the 16 *t*-Bu groups.

(72) CCDC 2010 Release.

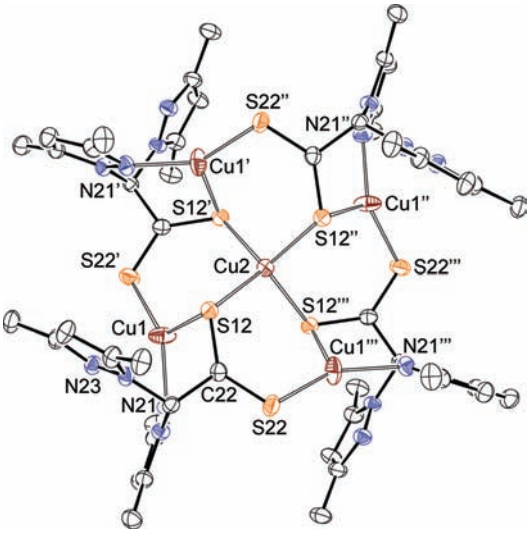

Figure 2. ORTEP drawing of $[Cu_5(L)_4]BF_4$ at the 30% thermal ellipsoids probability level. The methyl groups of the *t*-Bu residues, the BF_4^- anion, and the hydrogen atoms are omitted for clarity. Symmetry codes: $' = y-1/2; 1/2-x; 1/2-z, '' = -x; 1-y; z, ''' = 1/2-y; 1/2+x; 1/2-z$.

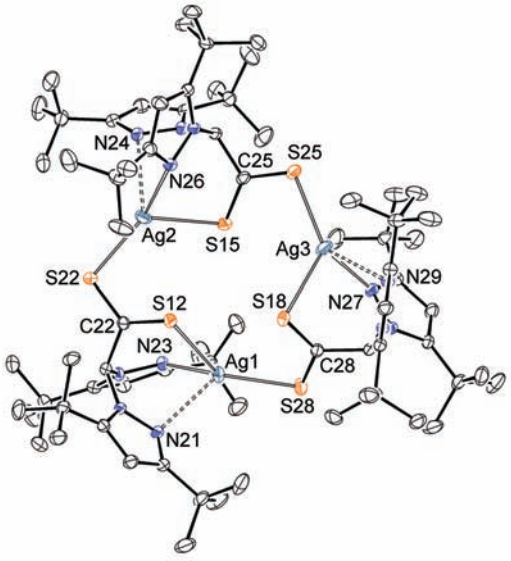

Figure 3. ORTEP drawing of $[Ag(L)]_3$ at the 30% thermal ellipsoids probability level. The hydrogen atoms are omitted for clarity.

The molecular structure of the silver complex is trinuclear (Figure 3). Each metal exhibits a geometry that is intermediate between trigonal pyramidal and tetrahedral; this geometry is achieved by the N_2S donor set of one ligand and by a sulfur atom of a second ligand. Two Ag−N bond distances are observed; one bond is significantly longer than the other (range 0.10−0.28 Å) and may be responsible for the distortion from the ideal trigonal planar geometry. Each silver atom lies out of the trigonal NS_2 planes by 0.41 Å (Ag(1)), 0.32 Å (Ag(2)) and 0.26 Å (Ag(3)), respectively, and points toward the apical nitrogen atom. Similar to the copper complex, both sulfur atoms in the $-CS_2^-$ group of the ligand are bound to a metal. The three bridging sulfur atoms are located at the periphery of the $Ag_3C_3S_6$ dodecatomic ring, whereas the chelating sulfur atoms point toward the center of the molecule, which form an irregular S_3 triangle with sides

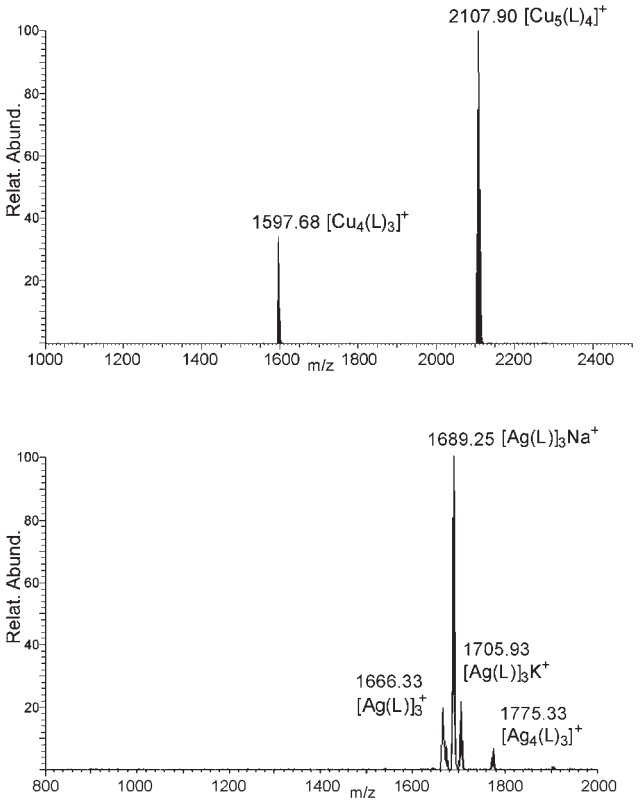

Figure 4. ESI-MS spectra of $[Cu_5(L)_4]BF_4$ and $[Ag(L)]_3$ dissolved in methanol.

that measure 4.11 Å, 3.75 Å, and 3.43 Å, respectively. The distance between these sulfur atoms and their centroid is in the 1.96−2.36 Å range.

Solution Studies. To confirm the presence of oligonuclear species in solution, we have performed ESI-MS and ^1H NMR experiments on $[Cu_5(L)_4]BF_4$ and $[Ag(L)]_3$ crystals dissolved in methanol and CD_2Cl_2, respectively. According to ESI-MS experiments, the peaks in the profile of the copper complex confirm the presence of the pentanuclear $[Cu_5(L)_4]^+$ cation (2107.9 m/z) as well as the presence of a tetranuclear species $[Cu_4(L)_3]^+$ (1597.6 m/z) (Figure 4). The ESI-MS technique provides detailed information on the species present in solution; however, some ambiguities remain as to whether the experimental conditions influence the peak intensities and the fragmentation pathways. This is particularly evident in the present case because the tetranuclear species may be a unique species or the result of fragmentation of the pentanuclear complex. To resolve this uncertainty, a detailed ^1H NMR investigation was performed on $[Cu_5(L)_4]BF_4$ (298 K) in CD_2Cl_2 solution. Two sets of signals are evident, which is consistent with the presence of at least two species (Figure 5). According to a ^1H NMR dilution titration (concentration range 0.005−0.0001 M, Supporting Information), one of the two sets of signals becomes predominant over the other during dilution or concentration of the solution. This result suggests that the two species are in equilibrium. A plausible explanation for this result is that the signals occurring at high concentration are those of the $[Cu_5(L)_4]^+$ entity, whereas those signals prevailing after dilution can be assigned to a species of lower nuclearity, which is presumably the tetranuclear complex

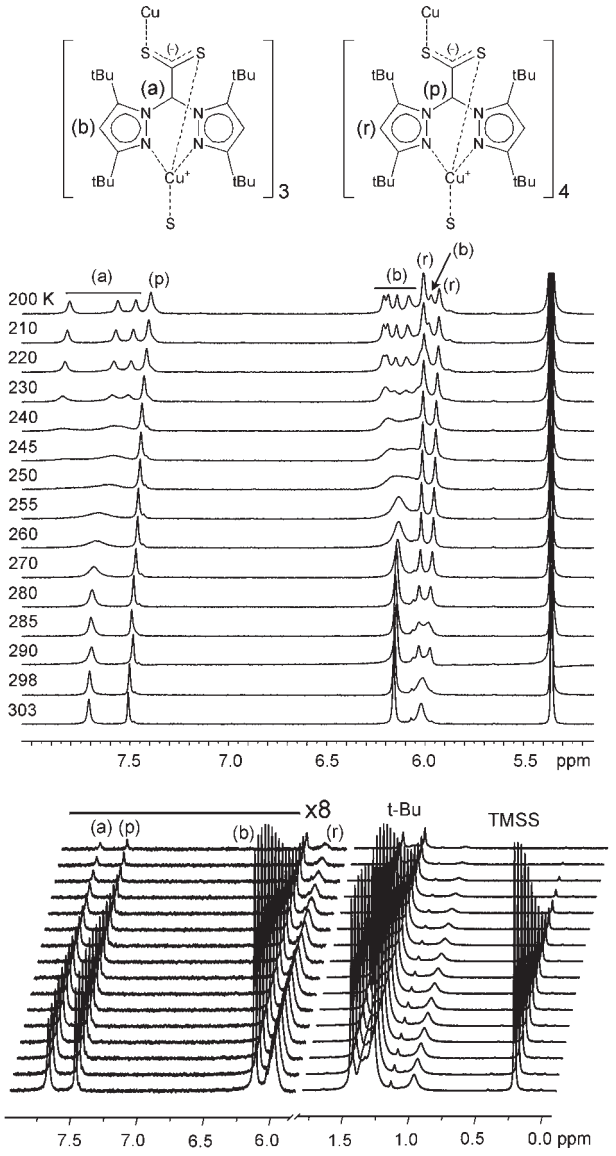

Figure 5. Top, variable temperature ^{1}H NMR spectra of $[Cu_5(L)_4]BF_4$ ($[Cu_4(L)_3]^+/[Cu_5(L)_4]^+$ ratio of 1/0.6). Bottom, stacking plot of ^{1}H PGSE NMR spectra for the same solution at room temperature (295 K) using the internal reference tetrakis(trimethylsilyl)silane (TMSS). Solvent: CD_2Cl_2. The intensity in the 6−8 ppm region has been increased 8-fold for clarity.

observed in the ESI-MS spectrum. This is further confirmed by ^{1}H PGSE NMR experiments for a solution in which both species were present in nearly equivalent quantity. This analysis confirms that both entities are relatively large because the hydrodynamic volumes (V_H) measure 2630(20) Å^3 and 2330(30) Å^3, respectively (Table 5). A comparison of the molecular volumes calculated using different methods suggests that the larger species corresponds to the pentanuclear complex $[Cu_5(L)_4]BF_4$ seen in the X-ray structures. The actual hydrodynamic volume is intermediate between the V_{vdW} and the solvent-excluded volume V_{SE} and is very close to the volume calculated by taking into account the occupancy of the unit cell (Table 5). The second species is slightly smaller, and it is reasonable to suggest that it corresponds to the tetranuclear complex. A proper structural assignment for this species used the structure of $[Ag(L)]_3$ as a model for a copper trinuclear entity via simple substitution of the metal ions, and the

Table 5. Hydrodynamic Volumes (V_H) of $[Ag(L)]_3$, $[Cu_4(L)_3]^+$, and $[Cu_5(L)_4]BF_4$ Species in CD_2Cl_2, and the van der Waals (V_{vdW}), Solvent-Excluded (V_{SE}) and X-ray ($V_{X\text{-}ray}$) Volumes, Determined As Described in the Text

	V_H (Å^3)	V_{vdW} (Å^3)	V_{SE} (Å^3)	$V_{X\text{-}ray}$ (Å^3)
$[Ag(L)]_3$	1720(30)	1254	2096	2123
$[Cu_4(L)_3]^+$	2330(30)[a]			
$[Cu_5(L)_4]BF_4$	2630(20)	1629	2700	3012

[a] The V_H of $[Cu_4(L)_3]^+$ and $[Cu_5(L)_4]^+$ have similar values, and the V_H of $[Cu_4(L)_3]^+$ is greater than that of $[Ag(L)]_3$. The large V_H of $[Cu_4(L)_3]^+$ is most likely a consequence of the dynamic equilibrium involving the $[Cu_4(L)_3]^+$ and $[Cu_5(L)_4]^+$ species.[75,76]

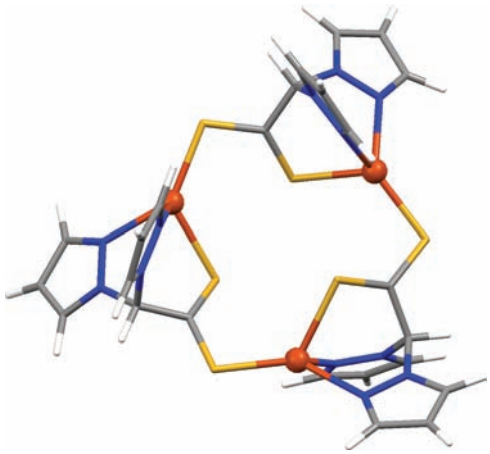

Figure 6. Optimized molecular structure of the $[Cu(L')]_3$ complex.[77] Density functional: B3LYP, basis set: Cu, S (lanl2dz) C,H,N (6-31G(d); in L′, the *t*-Bu of L are replaced by H atoms to save computational resources). Selected bond distances: Cu−N, 2.16−2.22 Å range; Cu−S_{bridge}, 2.31−2.32 Å range; Cu−$S_{chelate}$, 2.47−2.51 Å range.

geometry of the $[Cu(L')]_3$ model was optimized by DFT calculations (Figure 6). The three copper atoms of $[Cu(L')]_3$ are in a distorted tetrahedral environment, and the overall shape of the molecule resembles that of $[Ag(L)]_3$, but the pyrazole rings in $[Cu(L')]_3$ are symmetrically bound to the metal. Additionally, the inner triangular cavity delineated by three sulfur atoms in $[Cu(L')]_3$ may accommodate another Cu^+ ion because the distances from the centroid of this triangle to the sulfur atoms varies in the 2.04−2.29 Å range. The smaller species arising in solution may be either $[Cu(L)]_3$, which is analogous to the silver trimer, or $[Cu_4(L)_3]^+$, which is found in the ESI-MS spectrum.

Conclusive evidence supporting the structural assignment for the two sets of NMR signals associated with $[Cu_5(L)_4]BF_4$ and $[Cu_4(L)_3]^+$ is provided by the variable temperature experiment performed in the 200−303 K range (Figure 5). The signals (a) and (p) correspond to the central methinic proton for both complexes, and (b) and (r) are the signals of the central CH of the pyrazole ring. When the temperature is lowered, the "high dilution" singlets (a) and (b) split into three and six resonances, respectively. This change is consistent with loss of the 3-fold symmetry of the $[Cu_4(L)_3]^+$ complex at low temperature, which implies the loss of chemical equivalence of the three methinic and the six pyrazole protons. The absence of molecular symmetry between the three CuL units can be appreciated by examination of the optimized $[Cu(L')]_3$ structure. The kinetic parameters of the exchange process were determined from complete line shape analysis: $\Delta H^{\ddagger} = +42(2)$ kJ mol^{-1}, $\Delta S^{\ddagger} = -35(5)$ J

mol^{-1} K^{-1}.[73,74] The negative $\Delta S^{\ddagger}$ value obtained from this experiment suggests that it is most likely related to a non-dissociative fluxional mechanism that could be associated to the distortion of the $Cu_3C_3S_6$ dodecatomic ring (Figure 6).

The "high concentration" NMR signals (r) and (p) behave differently because they are associated with the pentanuclear species $[Cu_5(L)_4]BF_4$. On the basis of symmetry considerations made for the X-ray structure, the four CuL units are equivalent, but the two pyrazole rings within each unit are not equivalent. Binding of only one pyrazole to the metal could potentially explain the 2-fold splitting of the (r) signals observed at low temperature. The mutual partial rotation of the two pyrazoles with respect to each other, which results in continuous exchange of the coordination to the metal ion, makes them chemically equivalent at high temperature. The kinetic parameters of the fluxional process are $\Delta H^{\ddagger} = +57(2)$ kJ mol^{-1}, $\Delta S^{\ddagger} = -16(4)$ J mol^{-1} K^{-1}. In the Supporting Information, we report the VT spectra of two solutions containing different $[Cu_5(L)_4]BF_4$ concentrations, in which the $[Cu_4(L)_3]^+/[Cu_5(L)_4]^+$ ratios are ~9/1 and ~1/9, to better appreciate the splitting of the *t*-Bu resonances.

$[Ag(L)]_3$ exhibits more straightforward behavior in solution because it does not give rise to oligomer-oligomer equilibria. The ESI-MS confirms the presence of the silver cation $[Ag_4(L)_3]^+$ (Figure 4), which most likely originates during the ESI-MS ionization process via aggregation of the neutral $[Ag(L)]_3$ complex with Ag^+; however, the most abundant species are those deriving from the neutral $[Ag(L)]_3$ complex. In $[Ag(L)]_3$, the distances between the inner sulfur atoms and their centroid (1.96−2.36 Å) are too small for an optimal interaction with an additional Ag^+ ion; however, $[Ag(L)]_3$ may still be able to host a fourth metal ion in its center, for example, by a slight rotation of the CS_2^- groups that enlarges the inner cavity (Scheme 2). Another structural hypothesis for the $[Ag_4(L)_3]^+$ species consists of the interaction of the additional metal with one of the three S atoms that point toward the exterior of the complex (taking as reference the $[Ag(L)]_3$ structure), which are not buried by the *t*-Bu groups (Figure 3). The ^{1}H PGSE NMR experiment confirms the large size of the silver complex in solution, which is consistent with the X-ray structure (Table 5). The VT ^{1}H NMR experiments performed in the 298−230 K range do not indicate any signal multiplicity as found for the $[Cu_4(L)_3]^+$ complex. These results remain suggestive of even smaller values for the activation parameters for the silver trinuclear complex when compared to the copper species.

Scheme 2. Description of the Possible Structures for the Charged Species As Derived from the ESI-MS Analysis

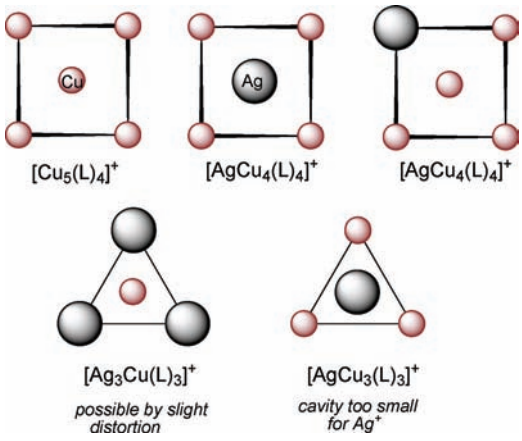

ESI-MS Titrations. On the basis of the structure of $[Cu_5(L)_4]BF_4$, the four metals at the exterior of the cluster are coordinately different from the central metal. In addition, the Cu−S distances for the inner metal suggest that other metal ions may be hosted by an empty $[Cu(L)]_4$ tetranuclear complex. To preserve or minimally affect the structure of the resulting $[MCu_4(L)_4]^{n+}$ species, M^{n+} should have a preference for tetrahedral geometry and should be small enough to avoid the collapse of the entire structure. Similar to BF_4^- in $[Cu_5(L)_4]BF_4$, the charge on M can also be compensated for by non-coordinating anions. We chose to employ Ag^+ for this study, and the formation of copper−silver adducts may be seen in Figure 7, which reports the change in the $[Cu_5(L)_4]^+$ mass spectrum as a function of the Ag^+ concentration. The peak at 2151.6 *m*/*z* corresponds to the $[AgCu_4(L)_4]^+$ cation, and the peak at 1641.5 *m*/*z* is a result of the fragmentation of the former, corresponding to $[AgCu_3(L)_3]^+$. This latter complex may already be present in solution; however, in this case, the structural considerations made for the $[Cu_4(L)_3]^+$ and $[Ag_4(L)_3]^+$ cations would no longer be valid. As shown in Scheme 2, the very small S_3 triangle formed by the $[Cu(L)]_3$ complex would be unlikely to host Ag^+; however, the additional Ag^+ ion may interact with the outer sulfur atoms. When the concentration of Ag^+ is increased to a $[Ag^+]/[[Cu_5(L)_4]BF_4]$ ratio > 5, the predominant species are $[AgCu_3(L)_3]^+$ at 1641.7 *m*/*z*, $[Ag_2Cu_2(L)_3]^+$ at 1685.7 *m*/*z*, $[Ag_3Cu(L)_3]^+$ at 1729.5 *m*/*z*, and $[Ag_4(L)_3]^+$ at 1775.5 *m*/*z*. According to the ESI-MS, these peaks originate from the parent ions of very low intensity that are found at the following *m*/*z* values: 2198.8 *m*/*z* ($[Ag_2Cu_3(L)_4]^+$), 2239.6 *m*/*z* ($[Ag_3Cu_2(L)_4]^+$), and 2284.3 *m*/*z* ($[Ag_4Cu(L)_4]^+$), respectively. When the Ag^+ concentration is increased, more extensive fragmentation of the tetranuclear species occurs because the most intense peaks are those associated with the mixed trinuclear species. Interestingly, the $[Ag_5(L)_4]^+$

(73) Sandstrom, J. *Dynamic NMR Spectroscopy*; Academic Press: London, 1982.
(74) Reich, H. J. *WINDNMR software: NMR Spectrum Calculations*, Version 7.1.11; 2005.
(75) Avram, L.; Cohen, Y. *J. Am. Chem. Soc.* **2005**, *127*, 5714–5719.
(76) Cabrita, E. J.; Berger, S. *Magn. Reson. Chem.* **2002**, *40*, S122–S127.
(77) Frisch, M. J.; Trucks, G. W.; Schlegel, H. B.; Scuseria, G. E.; Robb, M. A.; Cheeseman, J. R.; Montgomery, Jr., J. A.; Vreven, T.; Kudin, K. N.; Burant, J. C.; Millam, J. M.; Iyengar, S. S.; Tomasi, J.; Barone, V.; Mennucci, B.; Cossi, M.; Scalmani, G.; Rega, N.; Petersson, G. A.; Nakatsuji, H.; Hada, M.; Ehara, M.; Toyota, K.; Fukuda, R.; Hasegawa, J.; Ishida, M.; Nakajima, T.; Honda, Y.; Kitao, O.; Nakai, H.; Klene, M.; Li, X.; Knox, J. E.; Hratchian, H. P.; Cross, J. B.; Bakken, V.; Adamo, C.; Jaramillo, J.; Gomperts, R.; Stratmann, R. E.; Yazyev, O.; Austin, A. J.; Cammi, R.; Pomelli, C.; Ochterski, J. W.; Ayala, P. Y.; Morokuma, K.; Voth, G. A.; Salvador, P.; Dannenberg, J. J.; Zakrzewski, V. G.; Dapprich, S.; Daniels, A. D.; Strain, M. C.; Farkas, O.; Malick, D. K.; Rabuck, A. D.; Raghavachari, K.; Foresman, J. B.; Ortiz, J. V.; Cui, Q.; Baboul, A. G.; Clifford, S.; Cioslowski, J.; Stefanov, B. B.; Liu, G.; Liashenko, A.; Piskorz, P.; Komaromi, I.; Martin, R. L.; Fox, D. J.; Keith, T.; Al-Laham, M. A.; Peng, C. Y.; Nanayakkara, A.; Challacombe, M.; Gill, P. M. W.; Johnson, B.; Chen, W.; Wong, M. W.; Gonzalez, C.; Pople, J. A. *Gaussian 03*, Revision C.02; Gaussian, Inc.: Wallingford, CT, 2004.

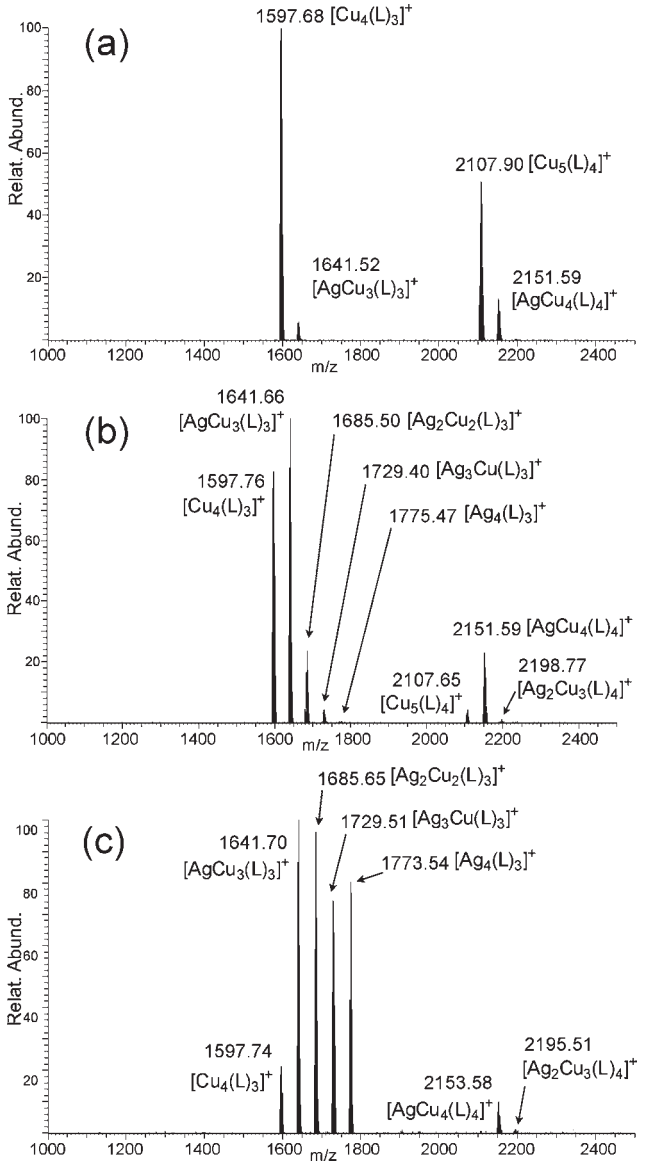

Figure 7. ESI-MS spectra collected at different $[Ag^+]/[[Cu_5(L)_4]BF_4]$ ratios: (a) 0.85; (b) 1.70; (c) 5.3.

species is never observed in any of the experimental conditions employed. This absence suggests that the highest nuclearity for the silver complex is three, as observed in the X-ray molecular structure.

Conclusions

We have investigated the coordination properties of the heteroscorpionate ligand bis(3,5-tertbutylpyrazol-1-yl)dithioacetate (L), which possesses a N_2S_2 donor set. Previous reports have shown that this type of ligand behaves as a N_2S donor with early transition metal ions because the dithioacetate group employs only one sulfur atom for metal binding.[44,70,71] By restricting rotation along the C−C axis, the *t*-Bu groups on the pyrazole ring of L direct the CS_2 moiety to a favorable position that chelates the metal center with a sulfur atom. The second sulfur is then available for binding an additional metal ion in a direction that is nearly perpendicular to the bis-pyrazole system. This steric control has important structural consequences for the nuclearity of the resulting complexes; oligonuclear species are preferentially formed with Li^+, Cu^+, and Ag^+. Co-crystallized THF molecules are present in the Li^+ crystals, but these molecules were not found to participate in the metal coordination, in contrast to previous reports for most structures in which Li^+ and THF are present. The lithium and silver complexes are trinuclear and form a trigonal internal cavity surrounded by three sulfur groups; in contrast, the copper complex is pentanuclear, and four equivalent CuL units delineate a regular tetrahedral site that is occupied by a fifth Cu^+ ion. This $[Cu_5(L)_4]BF_4$ complex, once dissolved, rapidly equilibrates with the tetranuclear species $[Cu_4(L)_3]^+$. According to the electroneutrality principle, the presence of both species in solution can be accounted for by the following equilibrium: $3[Cu_5(L)_4]^+ = [Cu(L)]_3 + 3[Cu_4(L)_3]^+$. The low temperature ^1H NMR spectrum suggests that only one set of signals is present for the tetranuclear entity, and the neutral $[Cu(L)]_3$ and charged $[Cu_4(L)_3]^+$ entities must rapidly exchange a labile copper ion. By employing Ag^+ instead of Cu^+, the highest nuclearity that is achieved is three (see ESI-MS data). This is also confirmed by the ESI-MS titration of a $[Cu_5(L)_4]BF_4$ solution with Ag^+, which demonstrates that the mixed trinuclear Cu^+/Ag^+ species predominates when the silver concentration increases.

In summary, we have explored the coordination capabilities of the new heteroscorpionate ligand bis(3,5-tertbutylpyrazol-1-yl)dithioacetate; the ligand was prepared as a lithium salt and behaved as a N_2S_2 donor with the two *soft* transition metal ions Cu^+ and Ag^+, exhibiting an ability to form stable oligonuclear structures.

Acknowledgment. This work was supported by the Ministero dell'Istruzione, dell'Università e Ricerca (Rome, Italy).

Supporting Information Available: Crystallographic information files (CIF) for $[Li(L)]_3 \cdot (2.25)THF$, $[Cu_5(L)_4]BF_4$ and $[Ag(L)]_3$. Cartesian coordinates of the optimized structures (B3LYP/lanl2dz-6-31G(d)) of the model complex $[Cu(L')]_3$. VT ^1H NMR spectra of $[Cu_5(L)_4]BF_4$ in CD_2Cl_2. This material is available free of charge via the Internet at http://pubs.acs.org.